Available online at www.sciencedirect.com

ScienceDirect

Procedia Structural Integrity 26 (2020) 285–292

Structural Integrity Procedia

www.elsevier.com/locate/procedia

The 1st Mediterranean Conference on Fracture and Structural Integrity, MedFract1

Investigation of the size effect and the fracture process on the uniaxial compressive strength of the banded Alfas porous stone

P. Nomikos[a], K. Kaklis[b,]*, Z. Agioutantis[c], S.Mavrigiannakis[d]

[a]*School of Mining & Metallurgical Engineering, National Technical University of Athens, Greece*
[b]*Department of Mining and Geological Engineering, Botswana International University of Science & Technology, Botswana*
[c]*Department of Mining Engineering, University of Kentucky, Lexington, Kentucky, USA*
[d]*School of Mineral Resources Engineering, Technical University of Crete, Greece*

Abstract

This paper focuses on the experimental and numerical investigation of the size effect and the fracture process on the uniaxial compression strength (UCS) of the banded Alfas porous stone. This natural building material excavated in Rethimnon, Crete, Greece often features two material bands with similar mineralogical properties, but different depositional characteristics and therefore different mechanical parameters. The experimental tests were simulated numerically using the Bonded Particle Model (BPM) available in the PFC2D code. The noticeable unusual increase of UCS with increasing specimen diameter as well as the strong influence of the weaker band on the mechanical behavior of the banded Alfas porous stone are confirmed by the numerical results. Future work will focus on the direct measurement of the weak/strong material band properties and will investigate the effect of the loading rate and boundary conditions on the mechanical response of the BPMs.

Keywords: Banded Alfas porous stone; building material; size effect; PFC2D; uniaxial compression strength tests

1. Introduction

Although the strength of small-size rock specimens can be studied and measured in the laboratory, a scaling law is typically needed to approximate the strength of the material when used in larger dimensions, i.e. strength of large

* Corresponding author. Tel.: +267 4931803; fax: +267 4900102.
E-mail address: kaklisk@biust.ac.bw

10.1016/j.prostr.2020.06.036

blocks or insitu strength. Scaling laws depend on the geomaterial as well as on the application field. One particular application field is the restoration of stone monuments, where researchers should determine suitable substitute materials that can be used in restoration projects as well as their behavior under different loading regimes (Vardoulakis and Kourkoulis (1998), Kourkoulis et al. (1999), Kourkoulis et al. (2000), Kourkoulis and Ninis (2001)).

The size effect has been extensively studied for concrete and several rock types. For example, Thuro et al. (2001), Yi et al. (2006), Viso et al. (2008) have investigated the effect of various factors such as size, shape, porosity, density on the UCS and the indirect tensile strength. In addition, recent studies have investigated the size effect for natural building stones (Kourkoulis and Ganniari-Papageorgiou (2010), Kourkoulis (2011), Kaklis et al. (2015)). The latter studies note that there are irregularities in the variation of the UCS as a function of diameter as observed through uniaxial compression tests. Specifically, previous uniaxial compression testing results as presented by Kaklis et al. (2015) clearly show that the UCS values increase with the diameter of cylindrical specimens. In conjunction with the presence of weaker bands in the Alfas porous stone, this variation remains an important subject that should be investigated with respect to the mechanical behavior of this material. This paper presents both experimental and numerical results of the size effect for the case of the banded Alfas porous stone.

The banded Alfas porous stone can be characterized as a transversely isotropic material due to its banded structure. Different sets of cylindrical specimens were prepared according to the International Society of Rock Mechanics (ISRM) specifications by varying their geometry in order to examine the size effect on the respective strength values.

The experimental tests were simulated numerically using the Bonded Particle Model (BPM) available in the PFC2D code. Heterogeneous, layered BPMs are constructed in PFC2D that contain one band of weak material. The PFC2D micro-parameters of the BPM were indirectly determined and the experimental fracture load and the failure pattern were compared to the numerical results.

The simulation results demonstrate that both the macro-mechanical response and the failure process can be modeled using BPMs. The strong influence of the weaker band on the mechanical behavior of the Alfas porous stone is confirmed. The differences between the numerical results and the macroscopic behavior are discussed.

2. Material and experimental procedure

2.1. Testing material

The banded Alfas porous stone is a natural building material excavated in Rethimnon, Crete, Greece. Its composition and physical properties are described in detail in previous studies by Kaklis et al. (2015) and Nomikos et al. (2020). The main characteristic is that often features two material bands with similar mineralogical but different depositional characteristics and therefore different mechanical parameters. The weak bands are typically characterized by a network of internal pores and surface vents.

2.2. Experimental procedure

An appropriate number of block samples for banded Alfas porous stone were collected from the quarry near the Alfas village in Rethimnon, Crete, and subsequently carefully checked to ensure the orientation of the rift plane and the absence of visible weaknesses. The size of these blocks was approximately 25x30x30 cm.

The cylindrical specimens were prepared by coring of the blocks normal to the plane of transverse isotropy in order to avoid variations in strength values, which could result from testing specimens with different orientations of the transverse plane.

Three sets of cylindrical specimens were prepared according to the ISRM specifications (Bieniawski and Bernede (1979)) for the uniaxial compression for banded Alfas porous stone (Fig. 1). The height h to diameter D ratio for the uniaxial compression test remained constant and equal to 2. In order to investigate the size effect, specimens were prepared with diameters $D = 54\ mm$, $D = 75\ mm$ and $D = 100\ mm$. Special care was taken to ensure that the two bases of the cylinders were parallel to each other and perpendicular to the longitudinal axis of the specimens. All experiments were carried out using a very thin film of vaseline jelly as lubrication between the bases of the specimens and the loading platens.

Load was applied using a stiff 1600 kN MTS hydraulic testing machine and a 500 kN load cell. The load was applied with a loading rate of 3 kN/s under load control mode for all uniaxial compression tests.

Fig. 1. A series of cylindrical specimens with different diameters for banded Alfas porous stone.

3. Numerical simulation

Distinct elements modeling of the uniaxial compression tests on banded Alfas porous stone specimens was performed by heterogeneous layered Bonded Particle Models (BPMs) created in the PFC2D, which include one band of weak material (Fig. 2).

3.1. Numerical specimen preparation and test execution

The PFC2D package utilizes an irregular packing of disk particles to represent the rock material. For the simulations of the current study, the particles are generated with their radii following a uniform distribution with a minimum radius R_{min} = 0.5 mm and a ratio of maximum to minimum radius R_{max}/R_{min}=1.5. The same random-number generator seed is used for the particle radii of all models irrespectively of their size. The particle assembly is created by generating disk particles within a rectangular area, with dimensions equal to the size of the numerical specimen, defined by confining walls that also act as boundary constrains. The particle assembly is initially cycled, while periodically reducing the kinetic energy of the system to zero, thus allowing the system to relax and eliminate large overlaps due to the generation procedure. Then the assembly is cycled to initial equilibrium.

After reaching initial equilibrium the lateral walls of the model are removed and bonds are applied between the particles in contact. The Linear Parallel Bond Model (Potyondy and Cundall 2004) is selected for the simulations of the current study. Different stiffness and strength micro-parameters are assigned to the bonds between particles belonging to the weak and the strong materials bands. Then, the BPM is ready to be numerically tested.

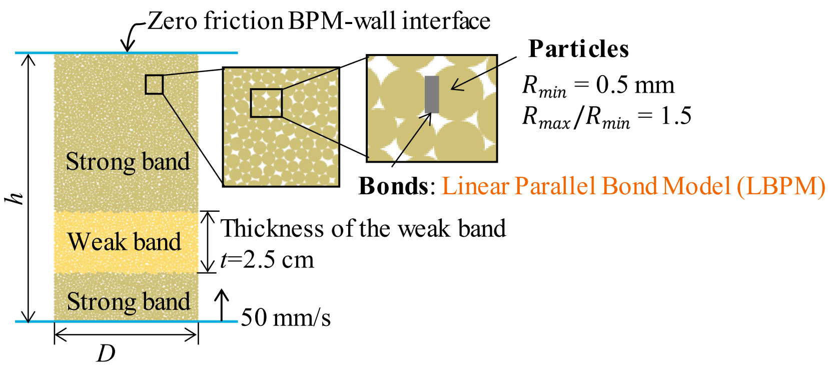

Fig. 2. Heterogeneous, layered BPM for simulation of the UCS tests of the banded Alfas porous stone specimens.

The numerical simulation of the uniaxial compression test is conducted as follows: The top wall that represents the top loading platen of an actual UCS test is fixed and the numerical specimen is loaded by specifying a constant velocity of 50 mm/s at the bottom model wall that represents the bottom loading platen of the UCS test. The friction between the loading walls and the specimens is set to zero in order to eliminate any end constraint effects in the numerical test.

Six BPM specimens are prepared in the PFC2D program for the simulation of the size effect of the banded Alfas porous stone specimens (Fig. 3). The numerical specimens have a 2:1 height-to-width ratio (h/D) and a width D=38, 54, 75, 100, 150 and 200 mm. The thickness of the weak material band remains constant and equal to t=2.5 cm and its distance to the bottom model wall is equal to 2.0 cm.

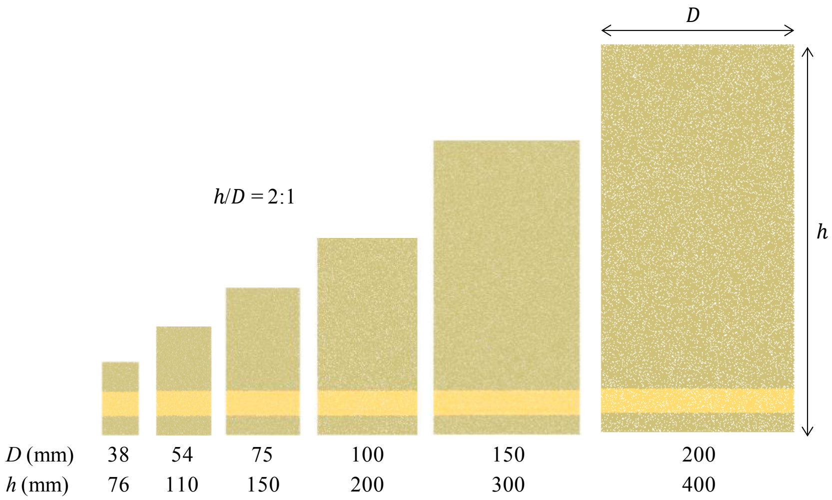

Fig. 3. Geometry of the BPMs for the simulation of the size effect of the banded Alfas porous stone specimens.

3.2. Contact model and BPM microparameters

The Linear Parallel Bond Model (LPBM) after Potyondy and Cundal (2004), is used as the bonding model for the BPMs of the current study. The micro-parameters that need to be specified are: the effective modulus of the contacts (E^*) and of the bonds ($\bar{E}^*$), the ratio of normal to shear stiffness ratio of the contacts ($\kappa^* = k_n/k_s$) and of the bonds ($\bar{\kappa}^* = \bar{k}_n/\bar{k}_s$), the normal ($\bar{\sigma}_c$) and shear ($\bar{\tau}_c$) strength of the bonds and the friction coefficient (μ) between the particles that is activated after the bond breakage.

The BPM needs to be calibrated so that its response to numerical testing matches the mechanical response of the rock material. The calibration process of the BPMs of the current study is described in detail by Nomikos et al. (2020). First, the uniaxial compressive strength (UCS_{est}) and the tangent elastic modulus ($E_{t,est}$) of the weak and strong bands of the Alfas porous stone were indirectly estimated by the Schmidt hammer rebound hardness and the P-wave velocity measurements (Fig. 4a). Then, the BPM microparameters were selected such that the uniaxial compressive strength (UCS_{PFC}) and the tangent elastic modulus ($E_{t,PFC}$) of the BPM, measured in a numerical UCS test in PFC2D (Fig. 4b), match the UCS_{est} and $E_{t,est}$ of the weak and strong material bands. The selected BPM micro-parameters are shown in Table 1.

4. Results and discussion

4.1. Experimental results

In the present work a total of 15 uniaxial compression laboratory tests for banded Alfas porous stone were completed in order to investigate the size effect. The experimental results for each diameter are presented in Table 2. Mean values of UCS are plotted against the diameter together with their standard deviation values. Fig. 5 shows clearly that UCS increases as the diameter size of Alfas stone specimens increases. A remarkable difference between the UCS for specimen size $D = 54\ mm$ and $D = 100\ mm$ is observed, which is about 27%.

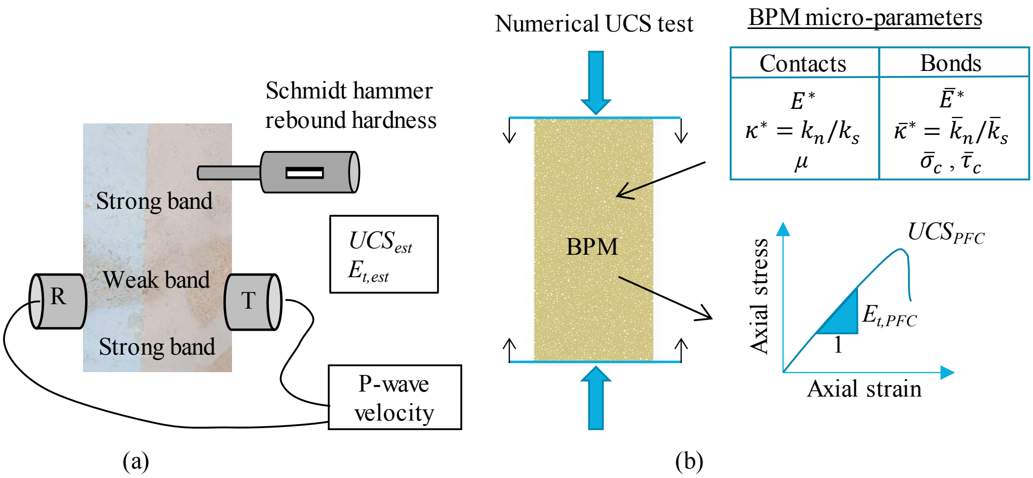

Fig. 4. (a) Indirect estimation of the weak and strong band material properties. (b) Calibration of the BPMs.

Table 1. BPM micro-parameters for the weak and strong material bands (Nomikos et al., 2020).

BPM micro-parameter	Strong material band	Weak material band
Stiffness ratio, $\kappa^* = \bar{\kappa}^*$	2.5	
Effective modulus, E^*=$\bar{E}^*$ (GPa)	14.07	5.32
Normal Bond Strength (NBS), $\bar{\sigma}_c$ (MPa)	20.28	6.0
Shear Bond Strength (SBS), $\bar{\tau}_c$ (MPa)	50.7	6.0
NBS/SBS	2.5	1.0
Friction coefficient between the particles (μ)	0.577	

Table 2. The experimental results of the uniaxial compression tests for banded Alfas porous stone.

h (mm)	D (mm)	Number of tests	Uniaxial compression strength (MPa)	St. deviation (MPa)
110	54	3	13.36	2.47
150	75	4	14.16	3.41
200	100	8	16.98	3.44

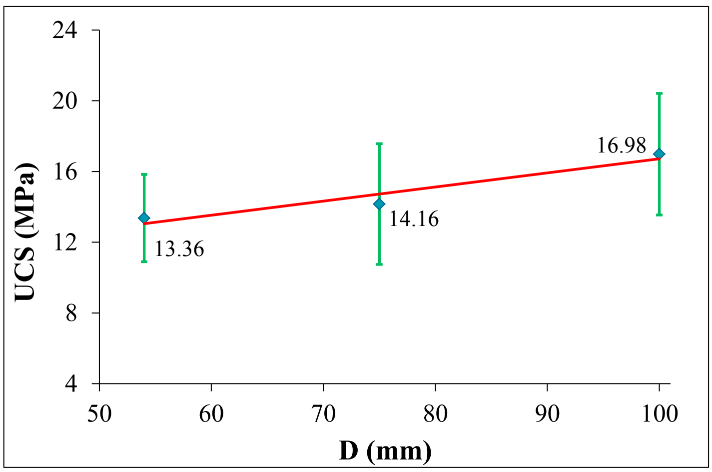

Fig. 5. Uniaxial compression strength with respect to the diameters of the specimens.

4.2. Numerical results

Fig. 6 shows the uniaxial compressive strength of the BPMs with respect to the width of the numerical specimen. Blue and red markers represent the numerical UCS of the homogeneous BPMs with strong and weak band material properties respectively. It is observed that the homogeneous BPMs with strong band material properties exhibit a slight reduction in strength with increasing specimen's width. For the homogeneous BPMs with weak band material properties an almost constant UCS is observed irrespectively of the specimen's width. The numerical results clearly indicate that the UCS of the banded BPMs increases as the width of the numerical specimen increases. This is attributed to the reduction of the percentage of the weak band material within the specimen.

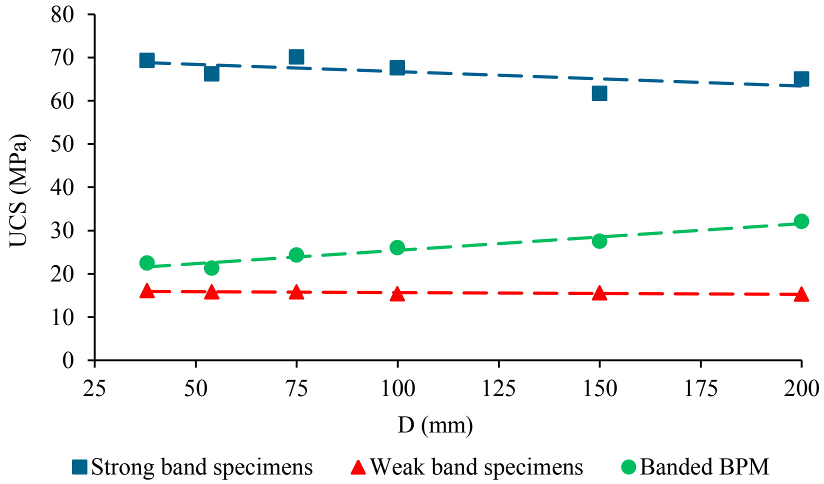

Fig. 6. Uniaxial compressive strength of the BPMs with respect to the specimen's width.

In Fig. 7 the axial stress – axial strain diagrams obtained from the numerical UCS tests of the banded BPMs are shown. It is observed that the stiffness of the banded BPMs increases with increasing specimen's width. This is also attributed to the reduction of the percentage of the weak band material within the numerical specimen.

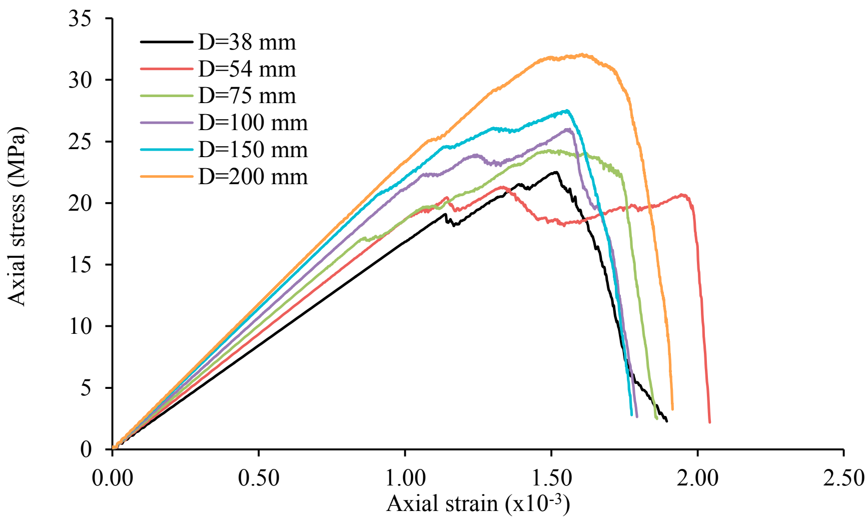

Fig. 7. Stress strain diagrams of the banded BPMs for the various BPM widths (diameters).

Fig. 8 presents the micro-cracking (i.e., bond breakages) observed in the banded BPMs after the end of the UCS test. Note that all tests were run until the post peak stress reached 10 % of the peak load. Shear microcracks (i.e., shear bond failure) are shown with red color, while tensile microcracks (i.e., tensile bond failure) are shown in black. It is observed that most of the specimen damage, consisting of both tensile and shear microcracks, is concentrated within the weak material band. In all the numerical models, tensile fracturing is observed in the adjacent strong material band during the last stages of the post peak loading of each specimen. This tensile fracturing extends towards the top loading platen for the model with D=38 mm and towards the bottom model wall for the rest of the numerical models. This fracture pattern matches the experimental observations for specimens (e.g., with D=54 mm) with a similar arrangement of the weak and strong material bands as discussed by Nomikos et al. (2020).

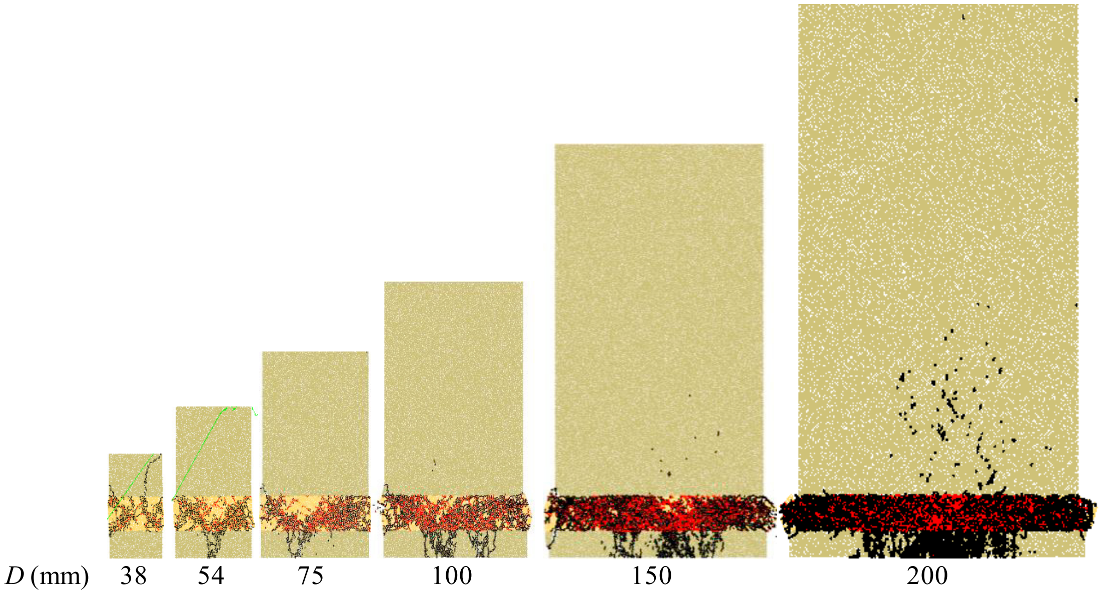

Fig. 8. Microcracking of the banded BPMs. Tensile and shear microcracks are shown with black and red colours respectively.

5. Conclusions

The size effect of the banded Alfas porous stone specimens under uniaxial compression is experimentally and numerically investigated. Cylindrical specimens of 2:1 height to diameter ratio and different specimen diameters were tested in the laboratory. The experimental results clearly show an increase of the uniaxial compressive strength with increasing specimen's diameter.

In order to investigate the size effect numerically, heterogeneous, layered BPMs with one band of weak material were constructed and numerically tested in the PFC2D code. BPMs with various widths and a 2:1 height to width ratio were examined. The thickness of the weak material band and its distance to the bottom wall of the model loading were kept constant and equal to 2.5 cm and 2.0 cm respectively. The BPMs were calibrated to match the indirectly estimated uniaxial compressive strength and elastic modulus of the strong and weak material bands. The numerical results indicate an increase of the UCS and stiffness of the BPMs with increasing the numerical specimen's width. This is attributed to the reduction of the percentage of the weak material within the specimen with increasing specimen's diameter. Further, fracturing of the BPMs is initiated within the weak material band, where most of the damage is concentrated. Both shear and tensile microcracks are formed within the weak band, while tensile fracturing is observed within the adjacent strong material band that mainly extends to the bottom wall of the model, when the numerical UCS simulations enter the post peak stage.

Fig. 9 presents the uniaxial compressive strength of the laboratory and the numerical specimens, normalized with respect to the UCS of the specimen with a diameter (width) of 54 mm. The increase of the normalized experimental and numerically simulated UCS with respect to the specimen's diameter/width is in good agreement. However, the size effect of the laboratory specimens is more pronounced.

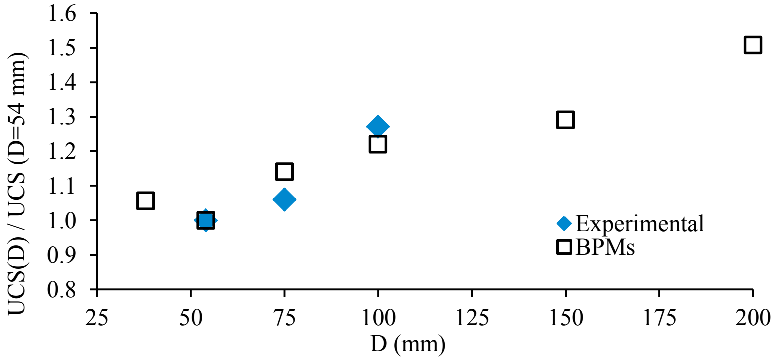

Fig. 9. Normalized UCS of the banded laboratory and numerical specimens

The numerical results indicate that both the macro-mechanical response and the failure process of the banded Alfas porous stone specimens can be modeled using BPMs. The strong influence of the weaker band on the mechanical behavior of the Alfas porous stone is confirmed. Furthermore, the numerical results confirmed the unusual increase of strength with increasing specimen diameter in the UCS tests of the Alfas porous stone. The differences between the numerical and experimental results may be attributed to the limitations of the model.

More experimental and numerical work is required to further investigate the size effect observed in this natural building material. Direct measurement of the weak/strong material bands mechanical properties should be performed along with a re-calibration of the BPMs to represent these properties. Finally, several aspects of the numerical models, such as the effect of loading rate and of the boundary conditions on the mechanical response of the BPMs, should be investigated.

References

Bieniawski, Z.T., Bernede, M.J., 1979. Suggested methods for determining the uniaxial compressive strength and deformability of rock materials. International Journal of Rock Mechanics and Mining Sciences & Geomechanics Abstracts 16(5), 135-140.

Kaklis, K., Maurigiannakis, S., Agioutantis, Z., Stathogianni, F., Steiakakis, E., 2015. Experimental investigation of the size effect on the mechanical properties on two natural building stones, Proceedings of 8th GRACM International Congress on Computational Mechanics. Volos, Greece.

Kourkoulis, S.K, Exadaktylos, G.E, Vardoulakis I., 1999. U-notched Dionysos Pentelicon marble in 3-point bending: the effect of nonlinearity, anisotropy and microstructure. Int J Fracture 98(3), 69-392.

Kourkoulis, S.K., Vardoulakis, I., Ninis N., 2000. Evaluation and theoretical interpretation of mechanical properties of porolithoi used in the restoration of the Epidaurean Asklepieion, In: Geological and Geotechnical Influences in the Preservation of Historical and Cultural Heritage, Ed. G. Lollino, Turin, Italy: CNDCI Publishing, I, 831–839.

Kourkoulis, S.K, Ninis, N.L., 2001. On selecting a compatible substitute for the Kenhcreae porous stone used in the Epidaurean Asklepieion, In: Aifantis EC, Kounadis AN, eds. Proc 6th national congress on mechanics. Thessaloniki, Greece, 348-356.

Kourkoulis, S.K., Ganniari-Papageorgiou E., 2010. Experimental study of the size- and shape-effects of natural building stones. Construction and Building Materials 24(5), 803-810.

Kourkoulis, S.K., 2011. An experimental study of the mechanical behaviour of the 'Conchyliates' shell-stone: some irregularities of the size effects. Strain 47(1), e344-e356.

Nomikos, P., Kaklis, K., Agioutantis, Z., Mavrigiannakis, S., 2020. Experimental characterization and numerical modeling of the fracture process in banded Alfas porous stone. Mat Design Process Comm., 1–15.

Potyondy, D.O., Cundall P.A., 2004. A Bonded-Particle Model for Rock. International Journal of Rock Mechanics & Mining Sciences 41(8), 1329-1364.

Thuro, K., Plinninger, R.J., Zah, S., Schutz, S., 2001. Scale effects in rock strength properties. Part 1: Unconfined compressive test and Brazilian test, ISRM Regional Symposium, EUROCK 2001, Rock Mechanics - a Challenge for Society, Espoo, Finland, 169-174.

Vardoulakis, I., Kourkoulis, S.K., Zambas, C., 1998. Modeling the mechanical behaviour of a conchyliates hellstone, In: The Geotechnics of Hard Soils-Soft Rocks, Eds. A. Evangelista & L. Picarelli, Rotterdam, Netherlands: Balkema, 911–922.

Viso, J.R., Carmona, J.R., Ruiz, G., 2008. Shape and size effects on the compressive strength of high-strength concrete. Cement and Concrete Research 38, 386-395.

Yi, S.T., Yang, E.I., Choi, J.C. (2006). Effect of specimen sizes, specimen shapes, and placement directions on compressive strength of concrete. Nuclear Engineering and Design 236, 115-127.